ACTA CHEMICA IASI, **34_2**, 405-442 (2026)
DOI: 10.47743/achi-2026-2-0017 *Article*

INFLUENCE OF DIISOCYANATE AND POLYOL–DIISOCYANATE RATIO ON MECHANICAL, THERMAL AND DEGRADABILITY PROPERTIES OF BIOPOLYURETHANE FOAMS FROM POULTRY WASTE

Viridiana Mancilla-Castillo[a], María C. Luján-Hidalgo[b], José H. Castañón-González[b], Zaira Domínguez[c], Teresa R. Ayora-Talavera[a], Beatriz C. Couder-García[a], Erik M. Polanco-Lugo[a], José M. Cervantes-Uc[d], Wilberth Herrera-Khao[d], Alejandro May-Pat[d], Rocío Meza-Gordillo[b*]

[a]*Centro de Investigación y Asistencia en Tecnología y Diseño del Estado de Jalisco, Subsede Sureste, Sierra Papacal-Chuburná Puerto, Parque Científico Tecnológico de Yucatán, 97302, Mérida, Yucatán, México*

[b]*Tecnológico Nacional de México/Instituto Tecnológico de Tuxtla Gutiérrez, Carr. Panamericana km 1080, 29050 Tuxtla Gutiérrez, Chiapas, México*

[c]*Instituto de Química Aplicada, Luis Castelazo Ayala s/n, Col. Industrial Ánimas, 91190, Xalapa, Veracruz. México*

[d]*Centro de Investigación Científica de Yucatán, A.C., Calle 43, No. 130. Col. Chuburná de Hidalgo, 97205, Mérida, Yucatán, México*

Abstract: Biopolyurethanes are versatile polymers commonly synthesized through polycondensation reactions between hydroxyl-functional compounds and diisocyanates, which contribute to the formation of soft and hard segments, respectively. Although vegetable oils are widely used as

* Rocío Meza-Gordillo, *e-mail:* rocio.mg@tuxtla.tecnm.mx

feedstocks for polyol production, animal fats such as chicken fat, offer a potentially sustainable alternative owing to their triglyceride composition. In this study, bio-based polyurethane foams were synthesized using a chicken oil polyol and three different diisocyanates: toluene diisocyanate (TDI), isophorone diisocyanate (IPDI), and hexamethylene diisocyanate (HDI). The effects of OH:NCO molar ratio and diisocyanate type on the physicochemical and thermal properties of the resulting foams were evaluated. IR spectroscopy confirmed the formation of urethane groups, with characteristic absorption bands at 3456 cm^{-1} (OH), 3299 cm^{-1} (N–H stretching), and 1723 cm^{-1} (C=O stretching). HDI based-foams exhibited the highest density, followed by TDI and IPDI based foams. Overall, HDI-based foams prepared at OH:NCO molar ratios of 1:5 and 1:6 ratios exhibited no significant difference in density, whereas those prepared at 1:4 differed significantly from both groups. In contrast, the density of TDI and IPDI based increased as the OH:NCO molar ratio changed from 1:4 to 1:6. Differential scanning calorimetry (DSC) revealed that the glass transition temperature (Tg) increased with higher OH:NCO molar ratios and with the use of higher-molecular-weight diisocyanates. Regarding biodegradation, HDI-based biopolyurethane foams exhibited greater susceptibility to degradation, possibly due to the linear aliphatic structure of the diisocyanate. These findings demonstrate that chicken oil represents a promising renewable feedstock for biopolyurethane synthesis, and that both diisocyanate type and OH stoichiometry significantly influence foam structure, physicochemical properties, and biodegradability.

***Keywords*:** Biopolymers; Polyols; Grease valorization; Sustainability; Bio-based materials

Introduction

Polyurethane foams (PUFs) are polymeric materials synthesized through the reaction between isocyanates and polyols, which are conventionally derived from non-renewable petroleum-based feedstocks.[1] Since their early development,[2] PUFs have gained considerable commercial importance because of their versatility and broad range of applications, including adhesive elastomers, coatings, resins, rigid and flexible foams, to insulation materials.[3] These characteristics have promoted their widespread use in industries such as construction, furniture, and packaging.[4,5] PUFs are classified as either flexible or rigid. Although both types are based on similar polyurethane chemistry, they differ in their degree of crosslinking,

intermolecular interactions, and density, depending on the nature and functionality of the reactants.[6,7] Hence, the chemical structure of polyurethane precursors plays a key role in determining the physicochemical, mechanical, and thermal properties of the resulting materials. Polyols may exhibit linear or branched structures, whereas diisocyanates may be aliphatic, cycloaliphatic, or aromatic. Therefore, understanding the structural characteristics of the available precursors is essential for tailoring foam rigidity through control of the resulting crosslinked network structure.[8,1]

The presence of aromatic rings in diisocyanates generally increases polyurethane rigidity by restricting segmental mobility, whereas aliphatic diisocyanates tend to produce more flexible materials with higher elongation but lower tensile strength.[9] Traditionally, the polyols and isocyanates used in polyurethane production have been predominantly derived from fossil-based feedstocks. Consequently, considerable research efforts have focused on developing renewable polyols to reduce dependence on fossil resources and improve the sustainability of PUFs.

Recently, bio-based polyols have been synthesized from a variety of renewable feedstocks,[10,11] including pine wood, sugarcane bagasse, marine oil, eucalyptus, and corn cobs.[12-17] However, most reported syntheses routes rely on vegetable oils as raw materials for the production of biobased polyurethanes.[18,19] More recently, increasing attention has been directed toward the valorization of animal-derived waste as an alternative source of lipids for polyol synthesis. Ramírez and collaborators (2022)[20] synthesized a polyol from waste poultry grease as a renewable lipid feedstock using a one-pot in situ process that combined epoxidation and subsequent ring-opening reactions. The synthesis conditions were optimized using a Box-Behnken response surface design, with temperature, catalyst concentration, double

bond-to-acetic acid molar ratio, and reaction time as the independent variables, and hydroxyl number as the response variable. The resulting polyol was subsequently used to synthesize polyurethane with isophorone diisocyanate (IPDI) at different polyol ratios, resulting in materials with distinct physical properties. Similar variations in polyurethane properties as a function of formulation were reported by Palle et al. (2023).[21] They investigated polyurethane films synthesized from *Acacia mangium* liquefied-wood polyol with polymeric methylene diphenyl diisocyanate (pMDI) at different OH:NCO molar ratios. Higher OH:NCO molar ratios resulted in increases in both the thermal degradation temperature and glass transition temperature (Tg). Prolonged heating also appeared to promote a higher crosslinking density in the *A. mangium*-based polyurethane films. Furthermore, increasing the OH:NCO molar ratio promoted urethane hydrogen-bonding interactions between the hard segments derived from pMDI and the soft segments derived from the polyol, thereby contributing to the increased rigidity of the films. Ristić et al. (2023)[22] synthesized polyurethane films via one-step polymerization using toluene diisocyanate (TDI) without a chain extender, along with various soft segments made from different macrodiols as soft segments including poly(D,L-lactide) (PDLLA) and polycaprolactone diol (PCL). Their findings demonstrated that the chemical composition of the soft segments directly influenced the properties of the resulting polyurethane films, highlighting the possibility of tailoring their characteristics for specific biomaterial applications. Overall, these findings indicate that polyol origin, diisocyanate type, and OH molar ratio are key factors governing the physicochemical, mechanical, and thermal properties of polyurethanes by affecting network architecture, crosslinking density, and intermolecular interactions between functional groups.

In this study, biopolyurethane foams were synthesized using a bio-based polyol derived from poultry waste and three structurally different diisocyanates (aromatic, cycloaliphatic, and aliphatic) at different molar ratios. The effects of diisocyanate type and molar ratio on the physicochemical and thermal properties of the resulting foams were evaluated.

Materials and methods

Raw material

Poultry fat residues were collected from local markets in Tuxtla Gutiérrez, Chiapas, México. The collected material was cleaned to remove feathers, viscera, cartilage, and skin, and subsequently stored at 4 °C, protected from light, for 24 h until use. The poultry waste fat was then placed in beakers and subjected to continuous direct heating at 90 °C for 6 h. The resulting poultry fat was allowed to cool and subsequently filtered through cotton cloth to remove residual solids.[23,24] The resulting poultry fat was purified by bleaching/deodorization and fractionation.[25] For the bleaching/deodorization process, the poultry fat was heated to 80 °C, and reagent-grade activated carbon was subsequently added at 3 % (w/w). The mixture was maintained under constant stirring for 15 min. Fractionation was then performed by cooling the poultry fat to 20 °C, followed by vacuum filtration to separate the liquid and solid fractions. The resulting liquid fraction was characterized and subsequently used for polyol synthesis.

Characterization of poultry fat

The extracted and purified poultry fat was characterized in terms of fatty acid profile, oxidative stability, kinematic viscosity, acid value, iodine value, and infrared spectroscopy. For fatty acid profile determination, the fatty acids were derivatized to their corresponding fatty acid methyl esters

(FAMEs) prior to gas chromatography mass spectrometry (GC-MS) analysis. Fatty acid derivatization was carried out by methylation. Briefly, 100 µL of poultry fat was mixed with 1 mL of 0.5 M NaOH prepared in HPLC-grade methanol. Hydrolysis was performed at 80 °C for 20 min under constant stirring. Subsequently, 1 mL of 14 % BF_3/MeOH was added, and the mixture was maintained at 20 °C under stirring for an additional 20 min. The resulting fatty acid methyl esters were extracted using 1 mL of hexane. A 1 µL aliquot of the hexane extract containing the FAMEs was injected into an Agilent 5975 inert XL GC-MS system (Agilent Technologies, Santa Clara, USA) equipped with a DB-WAX column (60 m × 0.25 mm × 0.25 µm). The initial oven temperature was maintained at 150 °C for 5 min and then increased to 210 °C at a rate of 30 °C min^{-1}. The temperature was subsequently increased to 213 °C at 1 °C min^{-1}, then to 225 °C at 20 °C min^{-1}, followed by a 20 min hold. Helium was used as the carrier gas at a flow rate of 1 mL min^{-1}. The injector temperature was set to 250 °C, and injections were performed in split mode using a 50:1 split ratio. Mass spectra were obtained by electron impact ionization at 70 eV. Compounds were identified by comparing the obtained mass spectra with those available in the HP Chemstation-NIST MS Library (A.00.1995).[24]

Oxidative stability was determined using an 873 Biodiesel Rancimat® instrument (Metrohm, Herisau, Switzerland) according to the EN 14112 standard.[26] A 3 g aliquot of the poultry fat was accurately weighed and transferred to the reaction vessel. The analysis was performed at 110 °C under a constant airflow of 10 $L \cdot h^{-1}$, and oxidative stability was expressed as the oxidation induction period (h). Kinematic viscosity was determined at 40 °C and 100 °C according to ASTM D445[27] using an SVM 3000® viscometer (Anton Paar, Graz, Austria). The functional groups present in

the poultry fat were identified by attenuated total reflectance Fourier-transform infrared (ATR-FTIR) spectroscopy using a Nicolet™ iS™10 FTIR spectrometer (Thermo Scientific, Waltham, USA) equipped with a diamond ATR accessory. Spectra were acquired over the range of 4000 to 500 cm^{-1} using 40 scans at a spectral resolution of 4 cm^{-1}.[28] The acid value was determined according to AOCS Method Te 1a-64 (2009).[29] Briefly, 85 mL of 95 % of ethanol was heated at 65 °C and neutralized prior to use by adding two drops of phenolphthalein indicator and titrating with 0.25 M KOH until a persistent pale pink endpoint was observed. Subsequently, 5 g of the poultry fat was accurately weighed into 250 mL Erlenmeyer flask and dissolved in the previously neutralized ethanol. Then, 0.5 mL of 1 % phenolphthalein in 95 % ethanol was added, and the mixture was titrated with 0.25 M KOH until the first pale pink color persisted for 30 s. The acid value was calculated using Equation 1:

$$\text{Acid value (mg KOH/g of sample)} = (V \times M \times 56.11) / P \quad (1)$$

where V is the volume of KOH used (mL), M is the molarity of the KOH (g/mol), P is the mass of the sample (g).

The iodine value was determined according to the Wijs method (AOCS Cd 1d-92, 1993b).[30] Briefly, 0.35 g of poultry waste was accurately weighed into a stoppered flask, followed by the addition of 20 mL of chloroform and 25 mL of Wijs reagent were added. The mixture was gently stirred and allowed to react in the dark for 1 h. Subsequently, 15 mL of 15 % (w/v) KI solution was added, and the mixture was thoroughly shaken. Then, 100 mL of distilled water was added while rinsing the stopper and the inner walls of the flask to ensure quantitative transfer of iodine into the reaction mixture. The mixture was titrated with 0.1N sodium thiosulfate ($Na_2S_2O_3$) solution under continuous stirring until the yellow color became

faint. Ten drops of 1 % (w/v) starch indicator solution were added, and the titration was continued until the blue color completely disappeared. A blank determination, without poultry fat, was performed in triplicate under the same experimental conditions. The iodine value was calculated according to Equation 2:

$$\text{Iodine value} = ((Vb - Vm) \times N \times 12.67) / Pm \quad (2)$$

where Vb is the volume of thiosulfate used in the negative control (mL), Vm is the volume of thiosulfate used in the sample (mL), N is the normality of the thiosulfate, 12.67 is the iodine equivalence, and Pm is the sample mass (g).

Polyol synthesis by epoxidation-hydrolysis reaction

For polyol synthesis, the poultry fat was subjected to epoxidation using acetic acid and hydrogen peroxide at stoichiometric ratios based on the molar amount of carbon-carbon double bonds (C=C) present in the fat. The molar amount of C=C double bonds was estimated from the experimentally determined iodine value according to Equation 3:

$$n(C=C) = (IY / (2 \times Mi \times 100)) \times P \quad (3)$$

where n(C=C) is the molar amount of carbon-carbon double bonds present in the poultry fat (mol), IY is the iodine value (g I_2 100 g^{-1}), Mi is the atomic molar mass of iodine (126.90 $g \cdot mol^{-1}$), and P is the mass of the poultry fat sample (g). The poultry fat was transferred to a three-neck flask, followed by the addition of acetic acid (CH_3COOH) and sulfuric acid (H_2SO_4), according to the specified molar ratio, with H_2SO_4 serving as the acid catalyst. The reaction mixture was continuously stirred at 350 rpm in an ice bath while maintaining the temperature below 20 °C. Hydrogen peroxide (H_2O_2) was then added dropwise over 15 min while maintaining the same temperature to control the exothermic reaction. After completion of H_2O_2 addition, the temperature was gradually increased to 80 °C, and the

reaction was maintained for 8 h. During this stage, the stirring rate increased from 350 to 700 rpm. After completion of the reaction, the reaction mixture was quenched by the addition of 5 % (w/v) sodium bicarbonate ($NaHCO_3$) solution and transferred to a separatory funnel. The organic phase was washed three times with 10 % $NaHCO_3$ solution, followed by washing with distilled water. Subsequently, 5 % (w/v) $NaHCO_3$ solution was added as required until a neutral pH was achieved. The pH was monitored using a sensIon 3 pH meter (HACH, Loveland, CO, USA) equipped with a model 51935-00 pH electrode. The organic phase was then treated with 20 % (w/w) anhydrous sodium sulfate to remove residual water; the drying agent was removed by filtration and the product obtained was the polyol.[31]

Characterization of polyol

The functional groups present in the poultry fat derived polyol were identified by ATR-FTIR spectroscopy using a Nicolet™ iS™10 FTIR spectrometer (Thermo Scientific, Waltham, MA, USA) as described above. The acid value of the polyol was determined according to the official AOCS method Te 1a-64 (2009), as previously described.[29] Prior to hydroxyl number determination, an acidity correction was performed to account for the contribution of acidic groups present in the polyol. Briefly, 2 g of polyol was accurately weighed into an Erlenmeyer flask, followed by the addition of 75 mL of pyridine, 75 mL of distilled water, and 0.5 mL of phenolphthalein indicator. The mixture was titrated with 0.1 N NaOH until a persistent, faint pink endpoint was reached. A blank determination was performed under the same conditions using the reagent mixture without the polyol. The acidity correction was calculated according to Equation 4:

$$\text{Acidity correction (AC)} = (A - B) \times N \times 56.1 / W \qquad (4)$$

where A is the volume of NaOH solution consumed in the polyol titration (mL), B is the volume consumed in the blank determination (mL), N is the normality of the NaOH solution, 56.1 is the molar mass of KOH ($g \cdot mol^{-1}$), and W is the mass of the polyol sample (g). The hydroxyl number of the poultry fat derived polyol was determined according to ASTM D4274-99.[32] 2 g of polyol were placed into a 250 mL stoppered Erlenmeyer flask, and 20 mL of acetylation reagent, prepared by dissolving 12.7 mL of acetic anhydride in pyridine to a final volume of 100 mL, was added. The mixture was vigorously stirred until the polyol was completely dissolved. The flask was heated in a water bath at 93 °C for 2 h and subsequently allowed to cool to room temperature. After cooling, 20 mL of distilled water was added while rinsing the stopper and inner walls of the flask to ensure the quantitative transfer of the reaction mixture. Additional distilled water was then added until the flask was approximately half full. Subsequently, 1 mL of 1 % phenolphthalein solution in pyridine was added, and the mixture was immediately titrated with 1 N NaOH solution until a persistent faint pink endpoint was reached. A blank determination was performed under the same experimental conditions without polyol. The hydroxyl number was calculated using Equation 5:

$$\text{Hydroxyl number} = [((B - A) \times N \times 56.1)] / W + AC \quad (5)$$

where A is the volume of NaOH solution used in the polyol titration (mL), B is the volume of NaOH solution consumed in blank titration (mL), N is the normality of NaOH solution, W is the mass of the polyol sample (g), and AC is the acidity correction (mg KOH g^{-1}) determined according to Equation 4.

Synthesis of bio-based polyurethane foams

Polyurethane foams (PUFs) were synthesized following the methodology by Ramírez Roblero (2022), with modifications. The poultry fat derived polyol obtained by epoxidation and hydrolysis was reacted with three structurally different diisocyanate (TDI), an aromatic diisocyanate; hexamethylene diisocyanate (HDI), and aliphatic diisocyanate and isophorone diisocyanate (IPDI), a cycloaliphatic diisocyanate. The polyol and each diisocyanate were combined at OH:NCO molar ratios of 1:4, 1:5, and 1:6 using methyl ethyl ketone (MEK) as solvent. Formulations containing IPDI or HDI were heated at 70 °C under continuous stirring for 5 min, whereas TDI based formulations were prepared at room temperature and mixed for 1 min. Immediately after mixing, the reaction mixtures were poured into 3×3 cm silicon molds and allowed to cure for 14 days. The resulting polyurethane foams were subjected to physicochemical and mechanical characterization.

The apparent density of the bio-based polyurethane foams was determined according to ASTM D1622.[33] Cube-shaped samples 3×3×2.5 cm were weighed using an analytical balance, and their volume were calculated from the measured dimensions. Three specimens from each formulation were analyzed, and the apparent density was calculated according to Equation 6:

$$D = Ws / V \quad (6)$$

where D is the apparent density (g/cm^3) Ws is the sample weight (g) and V is the sample volume (cm^3).

The thermal properties of the biopolyurethane foams were evaluated by differential scanning calorimetry (DSC) using a DSC 6000 differential scanning calorimeter (Perkin Elmer, Waltham, MA, USA). Samples were

heated from -20 °C to 350 °C at a heating rate of 10 °C min^{-1}, without a subsequent cooling cycle.

Soil degradation analysis of bio-based polyurethane foams

The soil degradation test was conducted under aerobic conditions according to the methodology described by Saha et al. (2021).[34] A total of 150 mg of each biopolyurethane foam was placed in 1 L containers filled with 1:1:1 (w/w/w) mixture of natural soil, commercial potting soil, and sand.

The soil pH was maintained between 6 and 8, and the relative humidity was maintained between 60 % and 80 % throughout the experiment. To maintain soil moisture, 1 mL of distilled water was added to the surface of each container every 7 days. The degradation experiment was conducted for 90 days. At the end of the exposure period, the foam samples were recovered from soil gently washed with distilled water to remove adhered soil particles and dried at room temperature for 24 h. The percentage of degradation of the biopolyurethane foams was evaluated based on the percentage of mass loss, calculated according to Equation 7:

$$\text{Percentage of degradation (\%)} = (mi - mf) / w_x \times 100 \qquad (7)$$

where mi is the initial mass of the sample (g), and mf is the final dry mass of the sample (g) after 90 days of soil exposure.

Changes in the chemical structure of the biopolyurethane foams after the soil degradation test were evaluated by ATR-FTIR spectroscopy using a Nicolet™ iS™ 10 FTIR spectrometer (Thermo Scientific, Waltham, MA, USA) under the experimental conditions described above.

Experimental design and statistical analysis

A completely randomized design was used to evaluate the effect of the OH:NCO molar ratio (1:4, 1:5, and 1:6) on the apparent density and

glass transition temperature (Tg) of the polyurethane foams. Statistically analyses were performed separately for each diisocyanate using one way analysis of variance (ANOVA) at a significance level of $p < 0.05$. When significant differences were detected, Tukey's multiple comparisons test was applied at a 95 % confidence level. Statistical analyses were performed using Statgraphics Centurion XVII software. All the experiments were performed in triplicate, and the results were expressed as mean ± standard deviation.

Results and discussion

Extraction and characterization of poultry oil

The yield of poultry fat obtained after the extraction and purification process was 69.70 %. This value was comparable to those previously reported by Hernández-Cruz et al. (2017)[25] who reported a yield of 60.71 %. Despite differences in the collection periods and geographical origins of the poultry waste, relatively high fat recovery yields were consistently obtained in the studies. These results suggest that poultry waste represents a promising and abundant lipid feedstock, with reported recovery yields exceeding 50 %. The high fat content of this residual material supports its potential valorization as a renewable raw material for lipid recovery and subsequent chemical conversion into value added products, such as biobased polyols.

Table 1 presents the physicochemical characteristics of extracted and purified poultry fat. The acid value was 1.01 mg KOH g^{-1} which is comparable to values reported for vegetable oils such as sacha inchi (*Plukenetia volubilis*)[35] oil and olive (*Olea europaea*) oil,[36] which reported acid values of 1.08 and 1.14 mg KOH g^{-1}, respectively. Both oils have been

used as renewable feedstock for polyol synthesis**.** The acid value is defined as the amount of potassium hydroxide (KOH), expressed in milligrams, required to neutralize the free fatty acids present in one gram of lipid. Therefore, the relatively low acid value obtained in this study indicates a low concentration of free fatty acid in the poultry fat, suggesting limited hydrolytic degradation of the triglycerides. This characteristic is favorable for its subsequent chemical conversion into a bio-based polyol, in particular, the carbon-carbon double bonds present in the unsaturated fatty acid moieties of the triglycerides provide reactive sites for chemical functionalization through epoxidation and subsequent ring-opening reactions, enabling the introduction of hydroxyl groups required for polyurethane synthesis. Thus, the value obtained in this study indicates a low concentration of free fatty acids in the poultry fat, suggesting limited hydrolytic degradation of triglycerides. This characteristic is favorable for its subsequent chemical conversion into a biobased polyol. Furthermore, the unsaturated fatty acid moieties of the triglycerides provide reactive sites for functionalization, enabling the introduction of hydroxyl groups required for polyurethane synthesis. The resulting hydroxyl functionality of the polyol can promote the formation of a crosslinked polyurethane network, which is particularly relevant to producing rigid foams.

Table 1. Physicochemical parameters of purified poultry oil.

Parameter	**Value**	
Acidic index (mg KOH g^{-1})	1.01	
Iodine index (g I_2 g^{-1} of sample)	83.2	
Oxidative stability (h)	1.23	
	40 °C	100 °C
Viscosity (mm^2 s^{-1})	36.76	8.09

The determination of the iodine value is particularly relevant for polyol synthesis, as it provides a quantitative measure of the degree of unsaturation in the lipid feedstock. These carbon-carbon double bonds serve as reactive sites for epoxidation and subsequent ring-opening reactions, enabling the introduction of hydroxyl groups required for polyurethane synthesis. The iodine value increases with the degree of unsaturation, as a greater number of double bonds allows more iodine to react with the lipid molecules. Hernández-Cruz et al., (2015)[24] reported an iodine value of 75.40 g I_2 100 g^{-1} of poultry fat used in biolubricant synthesis, which is comparable to the value obtained in this study (83.2 g I_2 100 g^{-1} sample). The iodine value obtained for poultry fat was slightly lower than those reported for olive oil (85 g I_2 100 g^{-1}) and castor oil (90 g I_2 100 g^{-1}), and lower than sunflower oil (135 g I_2 100 g^{-1}). These findings indicate that poultry fat contains a substantial proportion of unsaturated fatty acid moieties, providing reactive double bonds suitable for chemical functionalization. Therefore, poultry fat represents a promising lipid feedstock for biobased polyol synthesis through epoxidation and subsequent ring opening reactions.

The oxidative stability of the poultry fat evaluated in this study, expressed as the oxidation induction period, was 1.23 h. This value was comparable to those reported by Ramírez Roblero et al. (2022)[20] and Hernández-Cruz et al. (2015)[24], who obtained induction periods of 1.42 h and 1.38 h, respectively, for poultry fat. The relatively short oxidation induction period may be associated with the presence of unsaturated fatty acid moieties. This behavior highlights the importance of controlling oxidation during the storage and subsequent chemical processing of poultry fat.

Oxidative stability refers to the resistance of a lipid material to oxidation under vigorous conditions (110 °C and 10 $L \cdot h^{-1}$) and expressed as the oxidation induction period. Lipid oxidation involves the formation of primary oxidation products, mainly lipid hydroperoxides, through reactions involving unsaturated fatty acids. These compounds can be decomposed into secondary oxidation products such as aldehydes, ketones, and carboxylic acids which contribute to the development of rancidity. This relationship is consistent with the iodine value and the relatively short oxidation induction period obtained for poultry fat in the present study, suggesting that its unsaturated fatty acid content contributes to its susceptibility to oxidative degradation. Therefore, the relatively low oxidative stability observed in this study may be associated with the presence of unsaturated fatty acids in poultry fat, which are more susceptible to oxidative degradation. Regarding kinematic viscosity, poultry fat exhibited a value of 36.76 $mm^2\ s^{-1}$ at 40 °C, which was higher than the reported value for sunflower oil (28 $mm^2\ s^{-1}$ at 40 °C). This difference may be attributed to variations in fatty acid composition, particularly carbon chain length and degree of unsaturation, both of which influence intermolecular interactions and the flow behavior of lipid materials.

To further investigate the relationship between fatty acid composition and the physicochemical properties of poultry fat, its fatty acid profile was determined. Monounsaturated fatty acids (MUFAs) represented the predominant fraction (50.12 %), with oleic acid (18:1) as the major component, followed by saturated fatty acids (SFAs; 31.99 %), primarily palmitic acid (C16:0), and polyunsaturated fatty acids (PUFAs; 17.96 %), predominantly linoleic acid (C18:2). The combined proportion of

unsaturated fatty acids (68.08 %) highlights the presence of double bonds available for chemical functionalization. Compared with bovine and pork fats, which generally contain higher proportions of saturated fatty acids and tend to exhibit greater solid fat content at room temperature,[25] poultry fat has a higher proportion of unsaturated fatty acids, contributing to its predominantly liquid state under the conditions evaluated. This characteristic facilitates handling and processing, while the presence of double bonds provides reactive sites for chemical functionalization.

The functional groups present in poultry fat were characterized by ATR-FTIR spectroscopy (Figure 1). The spectrum exhibited a band at 3013.94 cm^{-1}, attributed to the stretching vibration of olefinic =C–H bonds in unsaturated fatty acids. Intense absorption band at 2919.10 and 2853.91 cm^{-1} were assigned to the asymmetric and symmetric stretching vibrations of Csp^3–H bonds, respectively. The strong band at 1741.59 cm^{-1} correspond to the ester carbonyl (C=O) stretching vibration characteristic of triglycerides, while the weak band at 1652.69 cm^{-1} was attributed to C=C stretching vibrations. Additionally, bands in the region of 1457–1370.48 cm^{-1} were associated with aliphatic C–H bending vibrations, whereas the absorption band at 1156.82 cm^{-1} was assigned to C-O stretching vibrations of ester groups with the triglyceride structure.[20]

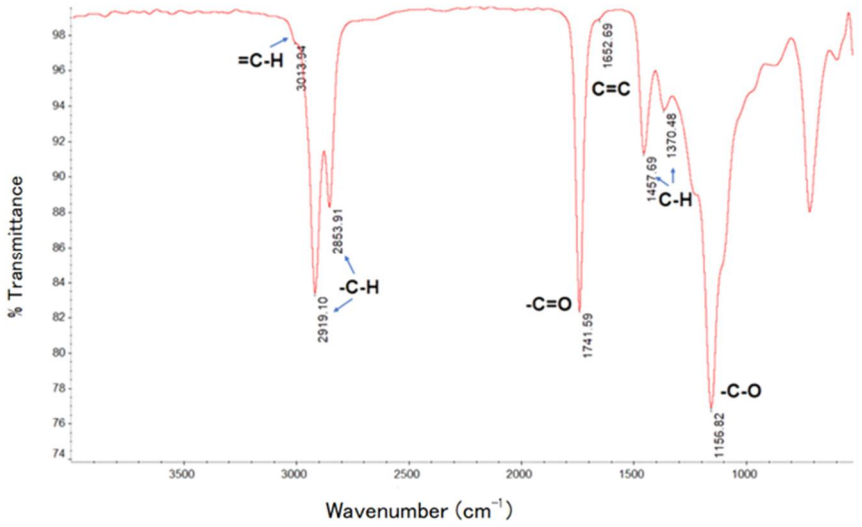


Figure 1. Fourier Transform Infrared (FTIR) spectrum of poultry fat oil, illustrating the functional groups present in the sample. The spectrum confirms the typical molecular structure of lipids, characterized by ester carbonyl groups, aliphatic hydrocarbon chains, and possible hydroxyl functionalities.

Characterization of polyol

The poultry fat derived polyol was synthesized through the epoxidation of double bonds present in the unsaturated fatty acid of triglycerides, using peracetic acid generated in situ from acetic acid and hydrogen peroxide, followed by oxirane ring-opening reactions to introduce hydroxyl groups. The acid value of the obtained polyol was determined, yielding 35.16 mg KOH/g, which is higher than that of the raw material (poultry fat, 1 mg KOH/g). This increase suggests a higher concentration of titratable acidic species in the synthesized polyol. Although the increase in acid value reflects changes in the chemical characteristics of the lipid material, the structural modifications were evaluated using ATR-FTIR. The IR spectrum (Fig. 2) exhibits a broad band at 3415 cm^{-1} attributed at the presence of hydroxyl groups, this absorption band provides evidence of hydroxyl formation during ring opening reaction of the epoxidized poultry

fat supporting the formation of the biobased polyol. The symmetric and asymmetric vibrations of methylene (-CH_2-) groups of the aliphatic fatty acids were identified at 2929 cm^{-1} and 2850 cm^{-1}, respectively. The intense band at 1722 cm^{-1} corresponds to the stretching vibration of ester carbonyl groups. Additionally, the bands at 1454, 1176, and 1096 cm^{-1} are assigned to the CH_2 and C–O–C stretching vibrations, respectively.

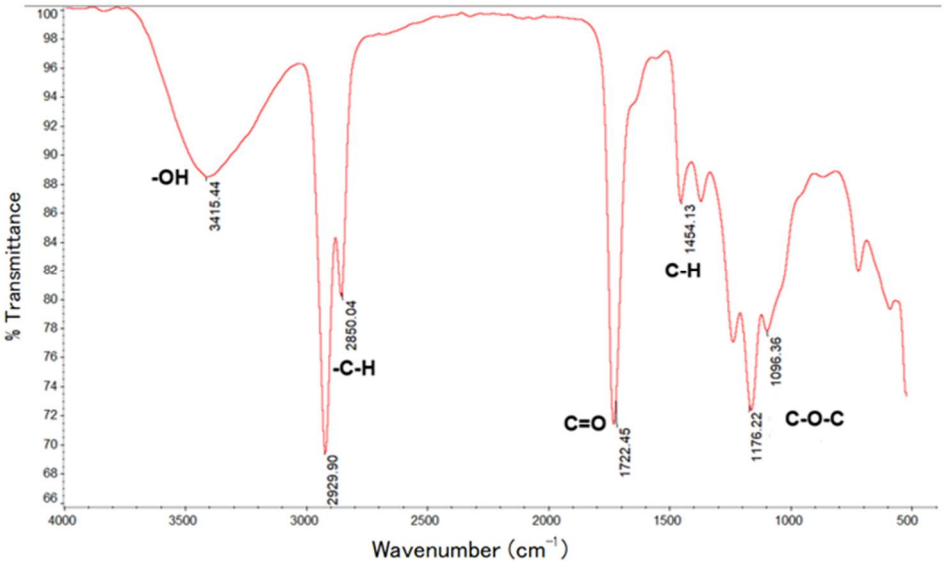


Figure 2. Fourier Transform Infrared (FTIR) spectrum of the polyol derived from the spectrum reveals the presence of hydroxyl functional groups, indicating the conversion of ester moieties into alcohol during the polyol synthesis process.

Synthesis and characterization of biopolyurethane foams

ATR-FTIR spectroscopy was performed to confirm the formation of urethane linkages in the synthesized polyurethane foams. Figure 3 presents the FTIR spectra of polyurethane foams synthesized with isophorone diisocyanate (IPDI) and toluene diisocyanate (TDI) at OH:NCO molar ratios of 1:4, 1:5, and 1:6. The characteristic absorption bands observed at 3299 cm^{-1} and 1723 cm^{-1} were attributed to N–H stretching vibrations C=O stretching vibrations of urethane groups, respectively. These spectral

features provide evidence of urethane linage formation in all synthesized, supporting the reaction between the hydroxyl groups of the biobased polyol and the isocyanate groups. However, signals detected at 2270 cm^{-1}, corresponding to the N=C=O stretching vibration of the diisocyanates, indicate the presence of unreacted isocyanate groups may be associated with the excess of isocyanate groups introduced during foam synthesis, particularly at higher OH:NCO molar ratios. Orojuela et al. (2021)[37] suggested that this behavior may be attributed to two factors. First, the hydroxyl groups in the synthesized polyol are located internal positions along the fatty acid chains rather than at terminal positions, which may introduce steric hindrance and reduce their accessibility and reactivity toward isocyanate groups. Second, the bulky triglyceride derived molecular structure, and the surrounding aliphatic chains may further restrict access to these hydroxyl groups, potentially limiting their reaction with diisocyanates during polyurethane formation. Hyung Lee et al. (2021)38 synthesized polyurethane foams using castor oil-based polyols. The FTIR spectra exhibited characteristic absorption bands at 3315 and 1705 cm^{-1}, corresponding to N–H and C=O stretching vibrations, respectively, providing evidence of the successful formation of urethane linkages. These findings are consistent with characteristic absorption bands observed in the present study, supporting the formation of urethane linkages in poultry fat derived polyurethane foams. However, a band at 2275 cm^{-1} was also identified, corresponding to the N=C=O stretching vibration, indicating the presence of unreacted NCO isocyanate groups in all the synthesized PU foams. This was expected, as an excess of NCO was added to react. The authors noted that the use of branched polyols may introduce steric hindrance, limiting the accessibility of hydroxyl groups for reaction with

NCO groups, and potentially reducing the extent of crosslinking. These structural constraints may also affect intermolecular interactions within the polyurethane network, ultimately reducing the mechanical strength of the resulting polyurethane.

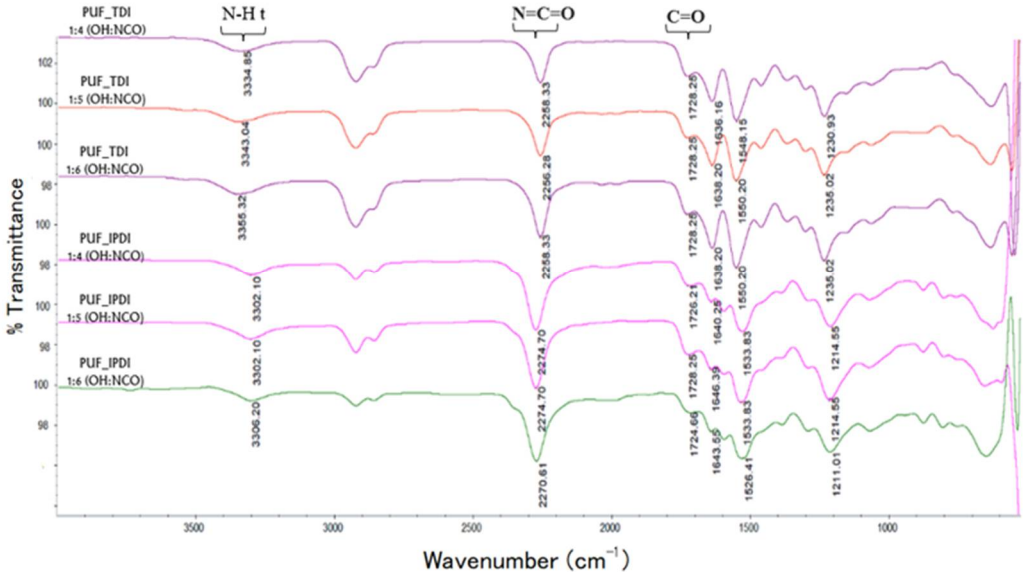


Figure 3. Fourier Transform Infrared (FTIR) spectrum of polyurethane foams synthesized using poultry fat-based polyol and two types of diisocyanates, toluene diisocyanate (TDI) and isophorone diisocyanate (IPDI), at molar ratios of hydroxyl to isocyanate groups (OH:NCO) of 1:4, 1:5, and 1:6. The spectra confirms the formation of urethane linkages, characteristic absorptions associated with N–H stretching, C=O stretching of the urethane group, and C–N and C–O vibrations within the polymer backbone.

The apparent density of the synthesized biopolyurethane foams was determined to evaluate the influence of the OH:NCO molar ratio used on this physical property (Figure 4). The apparent density of HDI based foams showed no statistically significant differences between OH:NCO molar rations of 1:5 and 1:6 ($p > 0.05$), whereas the 1:4 formulation differed significantly from both ($p < 0.05$). Similarly, IPDI foams exhibited comparable apparent densities at OH:NCO ratios of 1:5 and 1:6, while the 1:4 formulation showed a significantly lower density. In contrast, TDI-based foams exhibited no significant differences between the 1:4 and 1:5

formulations. However, the apparent density of the 1:6 formulation was significantly different than that of the 1:4 formulation. Overall, these findings indicate that the OH:NCO molar ratio influences the apparent density of poultry fat derived polyurethane foams, although the magnitude and statistical significance of this effect depend on the diisocyanate used. These findings are consistent with the results reported by Hoong et al. (2022),[39] who synthesized polyurethane foams from castor oil and different diisocyanates at different concentrations. Their results demonstrated that the apparent density of the resulting foams was influenced by diisocyanate content in the formulation, highlighting the role of precursor composition in determining the physical properties of the foams. Variations in diisocyanate content may influence polyurethane network formulation and foam expansion, potentially affecting cellular structure and, consequently, the apparent density of the resulting materials.

The type of diisocyanate also influenced the apparent density of the synthesized polyurethane foams, with differences observed among formulations prepared at the same OH:NCO molar ratio. Overall, HDI based foams exhibited the highest apparent density, followed by TDI and IPDI based foams (HDI > TDI > IPDI). These differences may be partially attributed to the molecular structure and steric characteristics of the diisocyanates, which influence the accessibility and reactivity of isocyanate groups during polyurethane.[40] HDI possess a linear aliphatic structure with two terminal isocyanate groups, providing relatively high accessibility for reaction with hydroxyl groups. In contrast, TDI contains two isocyanate groups attached to an aromatic ring at positions 2 and 4 relative to methyl substituent. The isocyanate group at position 2 experiences greater steric hindrance due to its proximity to the methyl group, whereas the group at position 4 is generally more accessible and exhibits higher reactivity toward hydroxyl groups. IPDI, a cycloaliphatic diisocyanate, contains two

chemically distinct isocyanate groups: one directly attached to a substituted cyclohexane ring, and another located on a methylene side chain. The steric environment surrounding these groups may influence their reactivity and consequently affect polyurethane network formation. These structural differences may contribute to variations in reaction kinetics, network development, and foam expansion, ultimately influencing the apparent density of the resulting foams.

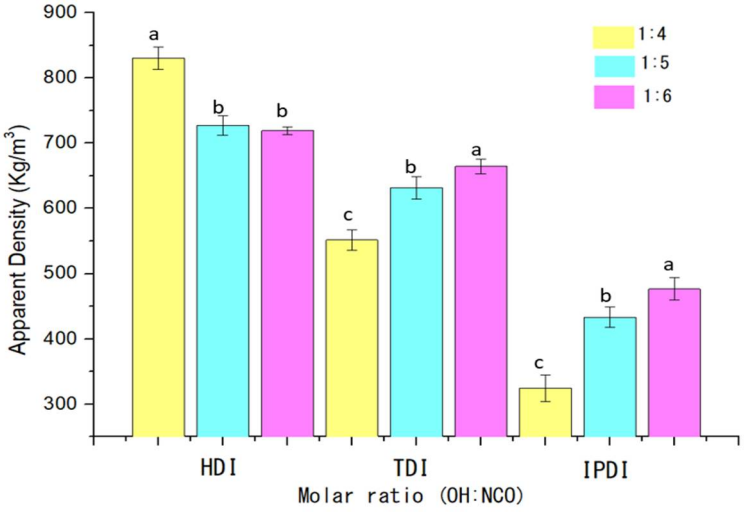


Figure 4. Effect of the OH:NCO molar ratio on the apparent density of polyurethane foams synthesized with poultry fat-based polyol. The figure illustrates how variations in the stoichiometric ratio between hydroxyl groups (OH) in the polyol and isocyanate groups (NCO) influence the foam density. As the NCO content increases, a denser crosslinked network is promoted (except for HDI), potentially leading to changes in foam expansion, cell size, and overall compactness.

The DSC thermograms of the biopolyurethane foams synthesized using different diisocyanates and OH:NCO molar ratio (Figure 5) showed thermal transitions associated with the glass transition temperature (Tg), crystallization temperature (Tc), and melting temperature (Tm). The presence of crystallization and melting transitions suggests the coexistence of amorphous and crystalline domains within the polyurethane structure, indicating a potentially semicrystalline morphology.

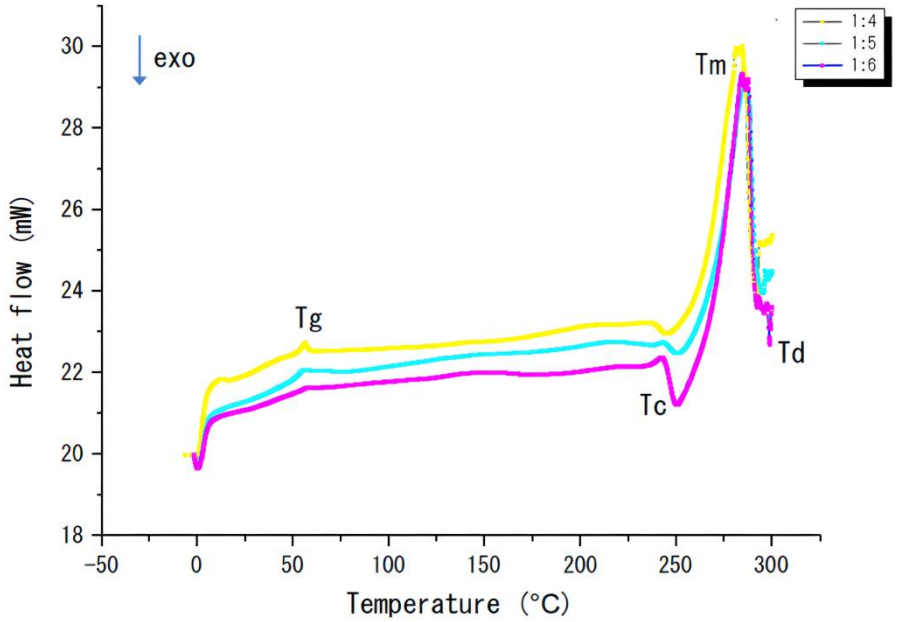


Figure 5. Differential Scanning Calorimetry (DSC) of biopolyurethane foams synthesized using poultry fat-based polyol and hexamethylene diisocyanate (HDI). The thermogram the glass transition temperature (Tg), crystallization temperature (Tc), melting temperature (Tm), and thermal decomposition temperature (Td). The Tg indicates the onset of segmental mobility in the soft segments of the polymer, while Tc and Tm reflect the semi-crystalline nature and phase transitions associated with hard segment ordering. The Td represents the thermal stability and degradation behavior of the foam, crucial for evaluating its performance under elevated temperatures.

An analysis of the differential scanning calorimetry assay of the biopolyurethanes revealed an increasing trend of Tg as the OH:NCO from 1:4 to 1:6 molar ratio (Table 2). This behavior suggests a progressive restriction of polymer chain mobility, potentially associated with changes in network structure and an increased degree of crosslinking. Additionally, hydrogen-bonding interactions between the C=O and N-H groups of urethane linkages may contribute to reducing segmental mobility and increased Tg values.[41] These intermolecular interactions can restrict molecular rearrangement, requiring higher temperatures for the transition from the glassy to the rubbery state. This trend was generally consistent

with the apparent density results, although apparent density is also influenced by cellular morphology and foam expansion.

Table 2. Analysis of transition (Tg), crystallization (Tc), and melting (Tm) temperatures as a function of OH:NCO molar ratio and diisocyanate type.

Molar ratio OH:NCO	Tg (ºC)	Tc (ºC)	Tm (ºC)
HDI (PM=168.2g/mol)			
1:4	64.4 ±0.17^{c}	245.7 ±0.0^{c}	282.5 ±0.0^{c}
1:5	72.5 ±0.16^{b}	250.9 ±0.0^{b}	284.3 ±0.0^{b}
1:6	75.5 ±0.16^{a}	252.3 ±0.0^{a}	285.3 ±0.0^{a}
TDI (PM=171.2g/mol)			
1:4	67.8 ±0.0^{b}	160.5 ±0.0^{c}	267.0 ±0.0^{c}
1:5	65.3 ±0.0^{c}	165.2 ±0.0^{b}	280.8 ±0.0^{a}
1:6	106.3 ±0.0^{a}	166.5 ±0.0^{a}	280.4 ±0.0^{b}
IPDI (PM=222.3g/mol)			
1:4	119.3 ±0.17^{a}	182.9 ±0.0	ND
1:5	114.9 ±0.16^{b}	ND	ND
1:6	114.9 ±0.16^{b}	ND	ND

ND: Not detected.

The molecular geometry and chemical structure of the diisocyanates may also influence polymer chain mobility, microphase organization, and thermal transition behavior. HDI, a linear aliphatic diisocyanate, contains a flexible six carbon chain that can facilitate segmental motion within the polyurethane network. In contrast, TDI and IPDI contain aromatic and cycloaliphatic ring structures, respectively, which may impose greater conformational restrictions on the polymer chains. Consequently, polyurethane networks incorporating these cyclic structures may exhibit higher Tg values than those based on HDI, depending on their composition, crosslinking characteristics, and intermolecular interactions.[42] These structural differences may also affect the organization of amorphous and crystalline domains, contributing to variations in the crystallization and melting behavior of the polyurethanes. Differences in thermal events

assigned to crystallization (Tc) and melting (Tm) may be associated with variations in hard segment organization. HDI based materials exhibited the highest temperatures for both transitions, suggesting a greater molecular packing capability. In contrast, the substituted aromatic structure of TDI and the asymmetric cycloaliphatic structure of IPDI may hinder the formation of ordered domains.

The mechanical performance of the synthesized polyurethane foams evaluated in term of maximum load (Figure 6), was influenced by both the diisocyanate type, HDI based foams exhibited the highest maximum load values across all formulations, followed by those synthesized with TDI and IPDI. For DI-based material, increasing the relative isocyanate content from an OH molar ratio of 1:4 to 1:6 resulted in a substantial increase maximum load, from approximately 18 kN to nearly 45 kN. This trend suggests that increasing the availability of isocyanate groups may promote changes in polyurethane network development that improve the load bearing capacity of the resulting foams. The linear aliphatic structure of HDI, characterized by two accessible terminal isocyanate groups, may facilitate urethane bond formation and contribute to the development of a mechanically effective network. However, the observed improvement cannot be attributed exclusively to increased crosslink density, as foam cellular morphology, apparent density, and structural uniformity may also influence mechanical performance. In contrast, TDI-based polyurethanes exhibited significantly lower maximum load values, reaching approximately 3 kN for the molar ratio 1:5, followed by a decrease at 1:6. This non monotonic behavior indicates that increasing the relative isocyanate content does not necessarily improve mechanical performance. The aromatic structure of TDI, together with the different steric environments and

reactivities of its two isocyanate groups, may influence polyurethane network formation and the resulting mechanical response. Variations in cellular morphology, network heterogeneity, and hard segment organization could also contribute to the observed differences. IPDI-based polyurethanes exhibited the lowest load values, remaining below 1 kN across the evaluated OH:NCO molar ratios. The bulky cycloaliphatic structure of IPDI and the distinct reactivities of its isocyanate groups potentially contribute to their limited load bearing capacity. The relatively small differences among the formulations suggest that increasing the relative isocyanate content did not produce a substantial improvement in maximum load under the synthesis conditions. Interestingly, IPDI based foams exhibited the highest glass transition temperatures but the lowest maximum load values, whereas HDI based foams showed substantially greater load bearing capacity. This contrasting behavior suggests that restricted segmental mobility as reflected by Tg does not necessarily translate into improved mechanical performance. Instead, the mechanical response of biopolyurethane foams appears to depend on the combined effect of polymer network, apparent density, and cellular morphology. These findings demonstrate that diisocyanate structure and OH:NCO molar ratio play important roles in determining the mechanical response of poultry fat derived biopolyurethane foams. HDI based formulations, particularly those prepared at a molar ratio of 1:6, exhibited the highest maximum load values, suggesting their potential suitability for applications requiring greater load bearing capacity. Furthermore, the contrasting thermal and mechanical behavior of IPDI and HDI based foams highlights the importance of considering both properties when selecting diisocyantes and polyurethane formulations for specific applications.

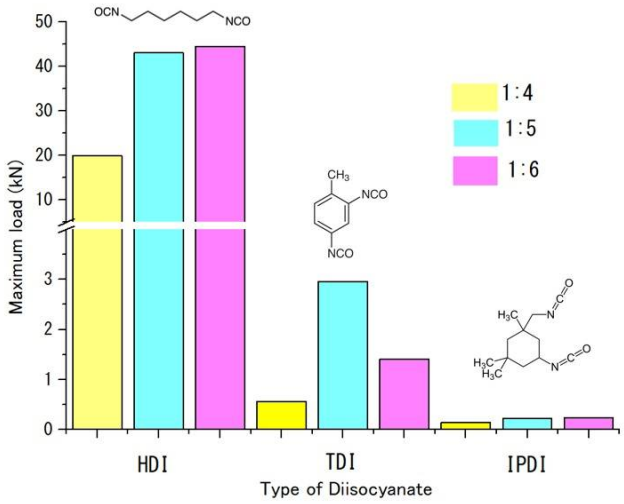


Figure 6. Mechanical performance of polyurethane foams synthesized with poultry fat-based polyol and various diisocyanates under different OH:NCO molar ratios. The figure presents key mechanical properties which reflect the structural integrity and load-bearing capacity of the foams. These properties are influenced by the degree of crosslinking, cell morphology, and the chemical nature of the polyol and isocyanate components.

Degradation of biopolyurethane foams

The mass loss of the synthesized biopolyurethane foams following soil exposure is presented in Figure 7. Among the evaluated formulations, HDI based foams prepared at OH:NCO molar ratios of 1:4 and 1:5 exhibited greater mass loss compared to those synthesized with IPDI and TDI, suggesting a higher susceptibility to deterioration under the experimental conditions. This behavior may be associated with the linear aliphatic structure of HDI, which provides greater conformational flexibility than the cyclic structures of IPDI and TDI. Such structural differences may influence polymer chain organization and the accessibility of susceptible bonds to degradation processes. Furthermore, formulations with relative isocyanate contents generally exhibited greater mass loss, suggesting that the OH:NCO molar ratio also influences the stability of the resulting polyurethane networks during soil exposure.

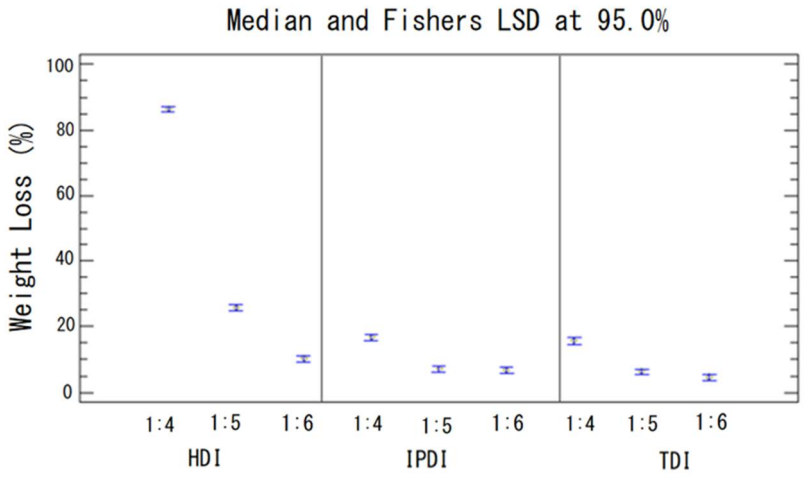


Figure 7. Weight loss degradation analysis of biopolyurethane foams synthesized from poultry fat-based polyol under controlled environmental conditions. The figure illustrates the percentage of mass loss over time, providing insight into the degradability and environmental stability of the materials. The degradation behavior is influenced by factors such as the chemical structure of the polyol, the type of diisocyanate used, and the crosslinking density of the polymer network. A higher rate of weight loss indicates greater susceptibility to hydrolytic, enzymatic, or microbial degradation processes.

Interestingly, HDI based foams exhibited higher apparent density and load bearing capacity than IPDI and TDI based formulations, while also showing greater mass loss under certain soil exposure conditions. This contrasting behavior suggests that improved initial mechanical performance does not necessarily imply greater resistance to environmental deterioration. The observed differences may be associated with variations in the accessibility of susceptible chemical bonds. Nevertheless, mass loss may arise from several processes, including polymer chain cleavage, leaching of soluble components, and physical deterioration. Changes in surface morphology and crystallinity may accompany these processes and affect the physical properties of the foams, although additional characterization would be required to confirm such structural modifications.

Figures 8 and 9 show the ATR-FTIR spectra of the IPDI and TDI based polyurethane foams before and after soil exposure, respectively. A

decrease of the absorption bands intensities at 3334 cm^{-1} and 1724 cm^{-1}, assigned to N–H and carbonyl C=O stretching vibrations of urethane groups, respectively, was observed after soil exposure. This spectral change suggests modifications in the chemical environment or relative abundance of urethane functional groups, potentially resulting from chemical bond cleavage during the exposure period of urethane groups.[43] Such changes are consistent with possible hydrolytic degradation of urethane linkages, although variation in hydrogen bonding and surface composition may also influence the observed band intensities. Similar results are consistent with those reported by Lee et al. (2016)[44], who observed a reduction in the intensity associated with the N–H absorption bands during polyurethan degradation and attributed these changes to urethane bond hydrolysis, potentially leading to the formation of amin and hydroxyl containing products. Furthermore, Saha et al. (2021)[34] investigated the degradation of polyurethane foams synthesized from castor oil, (poly(3-hydroxybutyate) diol, and hexamethylene diisocyanate under soil exposure conditions. Their FTIR results revealed a decrease in the intensity of the C=O absorption band at 1730 cm^{-1}, accompanied by an increase in the intensity bands of 1080–1090 cm^{-1} after degradation. These changes were associated with alterations in carbonyl containing groups and an increased contribution from C-O stretching vibrations, consistent with possible hydrolytic transformations within the polyurethane structure. In the present study, the disappearance of the absorption band near 1260 cm^{-1} may indicate changes in C-O stretching vibrations associated with ester containing groups. Additionally, a slight increase in the intensity of the band at 1567 cm^{-1}, was observed. This region is commonly associated with N-H bending coupled with C-N vibrations in urethane groups, although contributions from amine containing degradation products can not be excluded. Taken together, these

spectral changes suggest chemical modifications affecting both urethane and ester containing structures during soil exposure.

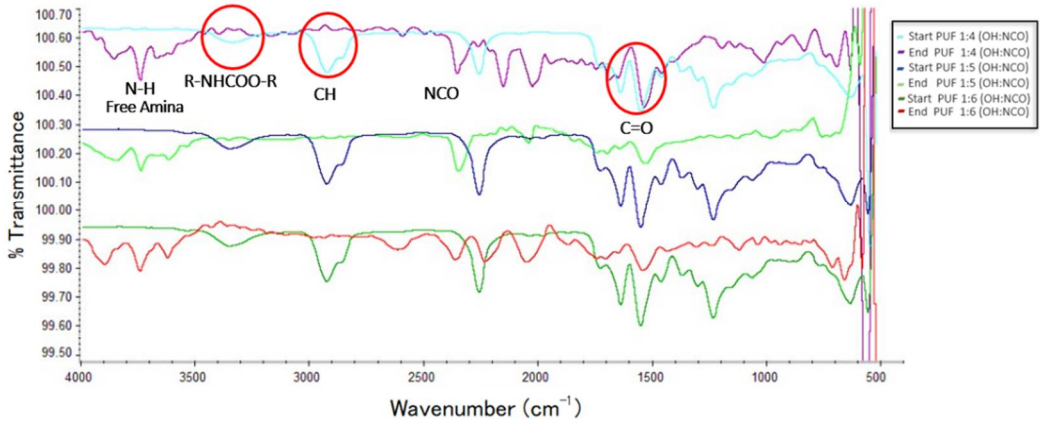


Figure 8. Fourier Transform Infrared (FTIR) spectrum of isophorone diisocyanate (IPDI)-based polyurethane foam following the degradation process. The spectrum highlights the chemical changes occurring in the polymer matrix because of hydrolytic, enzymatic, or environmental degradation. Notable variations in the intensity and position of characteristic absorption bands, such as reductions in urethane N–H and C=O stretching vibrations, indicate the cleavage of urethane linkages and breakdown of the polymer backbone.

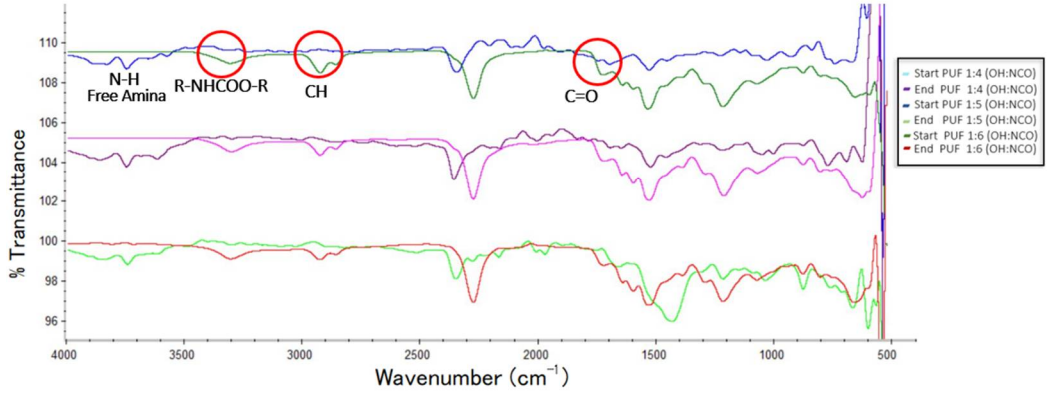


Figure 9. Fourier Transform Infrared (FTIR) spectrum of toluene diisocyanate (TDI)-based polyurethane foam after undergoing degradation. The spectrum reveals significant chemical modifications resulting from the breakdown of the polymer network. Decreases in the intensity of characteristic urethane bands, such as N–H stretching and C=O carbonyl vibrations, indicate cleavage of urethane bonds. Additionally, new or intensified absorption bands corresponding to hydroxyl, carboxyl, and amine groups suggest the formation of degradation products due to hydrolysis and chain scission.

Therefore, the probable degradation mechanism involves hydrolytic cleavage of urethanes through nucleophilic attack by water at the carbonyl carbon, potentially resulting in the formation of amine and hydroxyl containing species, with CO_2 release under reaction conditions. In parallel, ester groups present in the polymer structure may undergo hydrolysis (Figure 10), producing carboxylic acid and alcohol containing fragments. These reactions could contribute to polymer chain scission and the formation of lower molecular weight compounds, which may subsequently undergo further transformation under environmental conditions.

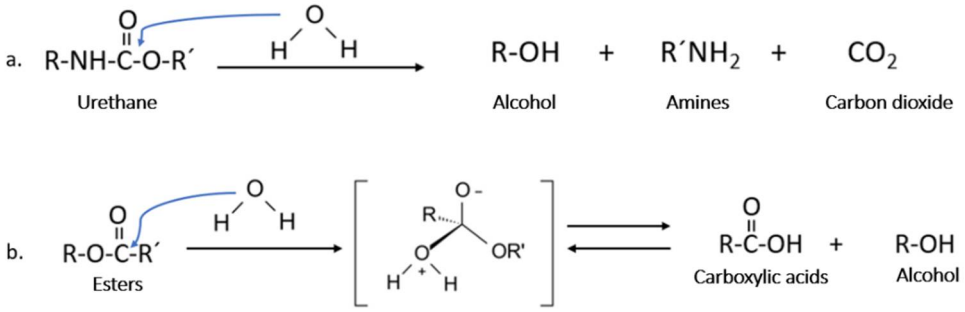


Figure 10. Schematic representation of the main hydrolytic degradation pathways in polyurethane (PU) foams. (a) Hydrolysis of the urethane bond, leading to the formation of amines and alcohols, which compromises the structural integrity of the polymer network. (b) Hydrolysis of the ester bond present in the soft segments of PU, resulting in the release of carboxylic acids and alcohols, contributing to polymer chain scission and material degradation. These mechanisms are especially relevant under conditions of high humidity and elevated temperature, significantly influencing the biodegradability and long-term stability of PU-based materials.

The observed FTIR changes, together with the mass loss recorded during soil exposure, support the occurrence of chemical and physical alterations in the synthesized polyurethane foams. The potential involvement of both urethane and ester linkages highlights the influence of polymer composition on environmental stability and provides a basis for

further investigation of the degradation behaviors of poultry fat derived polyurethane materials.

Conclusions

The results demonstrated the feasibility of converting poultry waste fat into biobased polyols through epoxidation and subsequent oxirane ring opening reactions, enabling the synthesis of biopolyurethane foams using different diisocyanates. Both diisocyanate structure and OH:NCO molar ratio influenced the physicochemical, thermal, and mechanical properties of the resulting materials. HDI foams generally exhibited the highest apparent density and load bearing capacity. In contrast, IPDI-based foams exhibited the highest glass transition temperatures, indicating greater restriction on polymer chain mobility. DSC analysis also revealed crystallization and melting transitions, suggesting the presence of semicrystalline domains within the polyurethane structure. During soil exposure, HDI-based foams exhibited greater mass loss than the corresponding IPDI and TDI based formulations. FTIR analysis revealed changes in absorption bands associated with urethane and ester containing groups, consistent with possible hydrolytic transformations, although the degradation mechanisms could not be conclusively established. However, these findings demonstrate that the selection of diisocyanate and OH:NCO molar ratio provides an effective approach for tailoring the properties of poultry fat derived biopolyurethane foams.

Acknowledgements

The authors thanks to National Council of Arts Humanities Science and Technology (México) [529084, VMM scholarship] and Mexican National Technologic/Tuxtla Gutiérrez Technologic Institute [grant number 14162.22-P].

Conflicts of interest

The authors of this article declare that they have no financial, professional or personal conflicts of interest that could have inappropriately influenced this work.

References

1. Serrano, L.; Rincón, E.; García, A.; Rodríguez, J.; Briones, R. Biodegradable polyurethane foams produced by liquefied polyol from wheat straw biomass. *Polymers* **2020**, *12*(11), 2646. https://doi.org/10.3390/polym12112646
2. Gupta, R.; Khol, P. (Eds.) *Polyurethane Chemistry: Renewable Polyols and Isocyanates*; American Chemical Society: Washington, DC, **2021**; Vol. *1380*.
3. Ateş, M.; Karadag, S.; Eker, A.; Eker, B. Polyurethane foam materials and their industrial applications. *Polym. Int.* **2022**, *71*(10), 1157 – 1163. https://doi.org/10.1002/pi.6441
4. Izarra, I.; Borreguero, A.; Garrido, I.; Rodríguez, J.; Carmona, M. Comparison of flexible polyurethane foams properties from different polymer polyether polyols. *Polym. Test.* **2021**, *100*, 107268. https://doi.org/10.1016/j.polymertesting.2021.107268
5. Wang, D.; Guo, J.; Su, M. Z.; Sun, J.; Zhang, S.; Yang, W.; Gu, X.; Li, H. The application of a novel char source from petroleum refining waste in flame retardant thermoplastic polyurethane. *Polym. Eng. Sci.* **2020**, *60*(5), 1029 – 1034. https://doi.org/10.1002/pen.25358
6. Gama, N.; Ferreira, A.; Barros Timmons, A. Polyurethane foams: Past, present and future. *Materials* **2018**, *11*(10), 1841. https://doi.org/10.3390/ma11101841
7. Somdee, P.; Ansari, M.; Marossy, K. Thermo-mechanical properties of flexible and rigid polyurethane (PU)/Cu composites. *Polym. Compos.* **2022**, *44*(1), 401 – 412. https://doi.org/10.1002/pc.27105
8. Fernández-Ángel, A.; Navarro, R.; Benito, E.; Guzmán, J.; Garrido, L. Properties of polyurethanes derived from poly (diethyleneglycol terephthalate). *Eur. Polym. J.* **2021**, *155*, 110576. https://doi.org/10.1016/j.eurpolymj.2021.110576

9. Veloso-Fernández, A.; Laza, J. M.; Ruiz-Rubio, L.; Martín, A.; Benito-Vicente, A.; Martín, C.; Vilas-Vilela, J. Advancing food packaging: Exploring cyto-toxicity of shape memory polyurethanes. *Materials* **2024**, *17* (19), 4770. https://doi.org/10.3390/ma17194770

10. Parcheta, P.; Datta, J. Environmental impact and industrial development of biorenewable resources for polyurethanes. *Crit. Rev. Environ. Sci. Technol.* **2017**, *47*(20), 1986 – 2016. https://doi.org/10.1080/10643389.2017.1400861

11. Furtwengler, P.; Avérous, L. Renewable polyols for advanced polyurethane foams. *Polym. Chem.* **2018**, *9*(32), 4258 – 4287. https://doi.org/10.1039/C8PY00827B

12. Lemaire, J.; Gardette, J.; Rivaton, A.; Roger, A. Dual photo-chemistries in aliphatic polyamides, bisphenol A polycarbonate and aromatic polyurethanes – A short review. *Polym. Degrad. Stab.* **1986**, *15*(1), 1 – 13. 10.1016/0141-3910(86)90002-9

13. Petrovic, Z.; Javni, I.; Ionescu, M. Biological oils as precursors to novel polymeric materials. *J. Renew. Mat.* **2013**, 167 – 186. https://doi.org/10.7569/JRM.2013.634112

14. Vega-Baudrit, J.; Delgado-Montero, K.; Madrigal-Carballo, S. Biodegradable polyurethanes from sugar cane biowastes. *Cellul. Chem. Technol.* **2011**, *45*(7-8), 507 – 514.

15. Czlonka, S.; Strakowska, A.; Pospiech, P.; Strzelec, K. Effects of chemically treated eucalyptus fibers on mechanical, thermal and insulating properties of polyurethane composite foams. *Materials* **2020**, *13*(7), 1781. https://doi.org/10.3390/ma13071781

16. Kosmela, P.; Hejna, A.; Suchorzewski, J.; Piszczyk, L.; Haponiuk, J. T. Study on the structure-property dependences of rigid PUR-PIR foams obtained from marine biomass-based biopolyol. *Materials* **2020**, *13*(5), 1257.

17. Kuranska, M.; Pinto, J. A.; Salach, K.; Barreiro, M.; Prociak, A. Synthesis of thermal insulating polyurethane foams from lignin and rapeseed based polyols: A comparative study. *Ind. Crops Prod.* **2020**, *143*, 111822.

18. Sabnis, A.; Kaikade, D. Recent advances in polyurethane coatings and adhesives derived from vegetable oil-based polyols. *J. Polym. Environ.* **2023**, *31*, 4583 – 4605. https://doi.org/10.1007/s10924-023-02920-z

19. Wibowo, E.; Papadopoulos, A.; Lubis, M.; Maulana, S.; Mardawati, E.; Iswanto, A. Eco-friendly and high-performance bio-polyurethane adhesives from vegetable oils: A review. *Polymers* **2024**, *16*, 1. https://doi.org/10.3390/polym16111613

20. Ramírez-Roblero, Y. *Síntesis y caracterización de biopoliuretanos elaborados a partir de grasa de pollo*. Tesis de Maestría, Instituto Tecnológico de Tuxtla Gutiérrez, Chiapas, México, **2022**.

21. Palle, I.; Lodin, V.; Yunus, A.; Lee, S.; Tahir, P.; Hori, N.; Antov, P.; Takemura, A. Effects of NCO/OH ratios on bio-based polyurethane film properties made from *Acacia mangium* liquefied wood. *Polymers* **2023**, *15*(5), 1154. https://doi.org/10.3390/polym15051154

22. Ristić, I.; Cakić, S.; Vukić, N.; Teofilović, V.; Tanasić, J.; Pilić, B. The influence of soft segment structure on the properties of polyurethanes. *Polymers* **2023**, *15*(18), 3755. https://doi.org/10.3390/polym15183755

23. Galeano, L.; Guapacha, M. E. *Aprovechamiento y caracterización de los residuos grasos del pollo para la producción de un biocombustible.* Informe técnico, **2011**. https://repositorio.utp.edu.co/entities/publication/1beda362-7e16-481a-95e5-e35bd5aa336e

24. Hernández-Cruz, M. del C. *Modificación de la viscosidad de grasa de pollo-biodiesel con aditivos, para la formulación de biolubricantes.* Tesis de Maestría, Instituto Tecnológico de Tuxtla Gutiérrez, Chiapas, México, **2015**.

25. Hernández-Cruz, M. C.; Meza-Gordillo, R.; Torrestiana-Sánchez, B.; Rosales-Quintero, A.; Ventura-Canseco, L.; Castañón-Gonzáles, J. Chicken fat and biodiesel viscosity modification with additives for the formulation of biolubricants. *Fuel* **2017**, *198*, 42 – 48. https://doi.org/10.1016/j.fuel.2016.12.039

26. EN 14112:2021. *Fat and oil derivatives – Fatty Acid Methyl Esters (FAME) – Determination of oxidation stability (accelerated oxidation).* Comité Européen de Normalisation: Brussels, **2021**. Último acceso: 01 mayo 2022.

27. ASTM D445-21. *Standard Test Method for Kinematic Viscosity of Transparent and Opaque Liquids (and Calculation of Dynamic Viscosity)*. ASTM International: West Conshohocken, PA, **2021**.

28. Jayavani, S.; Sunanda, S.; Varghese, T.; Nayak, S. Synthesis and characterizations of sustainable polyester polyols from non-edible vegetable oils: Thermal and structural evaluation. *J. Cleaner Prod.* **2017**, *162*, 795 – 805. https://doi.org/10.1016/j.jclepro.2017.06.040

29. AOCS. *Official Method Te 1a-64: Determination of Acid Value of Commercial Fatty Acids.* American Oil Chemists' Society, **2009**.

30. AOCS. *Cd 1d-92: Iodine Value of Fats and Oils, Cyclohexane-Acetic Acid Method.* American Oil Chemists' Society, **1993**.

31. Salimon, J.; Abdullah, B.; Yusop, R.; Salih, N. Synthesis, reactivity and application studies for different biolubricants. *Chem. Cent. J.* **2014**, *8*, 16. https://doi.org/10.1186/1752-153X-8-16

32. ASTM D4274-99. *Standard Test Methods for Testing Polyurethane Raw Materials: Determination of Hydroxyl Numbers.* ASTM International: West Conshohocken, PA, **1999**.

33. ASTM D1622-03:2010. Standard Test Method for Apparent Density of Rigid Cellular Plastics. ASTM International. Disponible en: https://www.astm.org/d1622-03.html

34. Saha, P.; Khomlaem, C.; Aloui, H.; Kim, B. Biodegradable polyurethanes based on castor oil and poly(3-hydroxybutyrate). *Polymers* **2021**, *13*(9), 1387. https://doi.org/10.3390/polym13091387

35. Rodríguez, G.; Squeo, G.; Estivi, L.; Berru, S.; Buleje, D.; Caponio, F.; Brandolini, A.; Hidalgo, A. Changes in stability, tocopherols, fatty acids and antioxidant capacity of sacha inchi (Plukenetia volubilis) oil during French fries deep-frying. *Food Chem.* **2020**, *340*, 127942. https://doi.org/10.1016/j.foodchem.2020.127942

36. Mahdi, S.; Azzi, R.; Abdellaoui, Z.; Bouziane, K.; Kadouci, F.; Mekahli, F.; Kalai, I.; Serhane, N. Assessment of chemical quality properties and phenolic content of different samples of Algerian olive oil. *Genet. Biodivers. J.* **2022**, *6*(1), 25 – 36. https://doi.org/10.46325/gabj.v6i1.194

37. Orjuela, C.; Bohórquez, Á.; Díaz, W.; Narváez, M.; Cadavid, P.; García, N. Polioles grasos: producción, retos y oportunidades para el sector del

aceite de palma. Corporación Centro de Investigación en Palma de Aceite (Cenipalma), **2022**.

38. Hyung Lee, J.; Hun Kim, S.; Wha Oh, K. Bio-based polyurethane foams with castor oil based multifunctional polyols for improved compressive properties. *Polymers* **2021**, *13*, 0576. https://doi.org/10.3390/polym13040576

39. Hoong, S.; Srihanum, A.; Devi, K.; Ain, N.; Mohd, N.; Kian, Y.; Din, N.; Noor, M. Low density rigid polyurethane foam incorporated with renewable polyol as sustainable thermal insulation material. *J. Cell. Plast.* **2022**, *58*, 485 – 503. https://doi.org/10.1177/0021955X211062630

40. Li, Y.; Luo, X.; Hu, S. Bio-based polyols and polyurethanes. New York, Dorecht, London: Springer, **2015**.

41. Rahman, M.; Zaman, J.; Yoon, M.; Hoque, M.; Tian, L.; Johir, M.; Wang, S.; Ahmed, M.; Choi, J.; Alam, M. Interaction chemistry of functional groups for natural biopolymer-based hydrogel design. *Mat. Sci. Eng. R: Rep.* **2023**, *156*, 100758. https://doi.org/10.1016/j.mser.2023.100758

42. Acik, B.; Acik, G.; Erdemi, H. Synthesis and characterization of bile acid, poly(ε-caprolactone) and L-lysine diisocyanate ethyl ester-based polyurethanes and investigation of their biodegradability properties. *Eur. Polym. J.* **2021**, *146*, 110247. https://doi.org/10.1016/j.eurpolymj.2020.110247

43. Chavarro Gomez, J. et al. Characterization of novel rigid-foam polyurethanes from residual palm oil and algae oil. *J. Mater. Res. Technol.* **2020**, *9*, 16304 – 16316. https://doi.org/10.1016/j.jmrt.2020.11.095

44. Lee, C. S.; Ng, W. S.; Chuah, C. H.; Cheng, S. F. Preparation and modification of water-blown porous biodegradable polyurethane foams with palm oil-based polyester polyol. *J. App. Polym. Sci.* **2017**, *97*, 65 – 78. 10.1016/j.indcrop.2016.11.066